

Performance enhancement of GaN metal–semiconductor–metal ultraviolet photodetectors by insertion of ultrathin interfacial HfO₂ layer

Manoj Kumar, Burak Tekcan, and Ali Kemal Okyay

Citation: *Journal of Vacuum Science & Technology A* **33**, 021204 (2015); doi: 10.1116/1.4905735

View online: <http://dx.doi.org/10.1116/1.4905735>

View Table of Contents: <http://scitation.aip.org/content/avs/journal/jvsta/33/2?ver=pdfcov>

Published by the AVS: Science & Technology of Materials, Interfaces, and Processing

Articles you may be interested in

High-performance AlGaIn metal–semiconductor–metal solar-blind ultraviolet photodetectors by localized surface plasmon enhancement

Appl. Phys. Lett. **106**, 021112 (2015); 10.1063/1.4905929

Performance improvement of GaN-based ultraviolet metal–semiconductor–metal photodetectors using chlorination surface treatment

J. Vac. Sci. Technol. B **30**, 031211 (2012); 10.1116/1.4711215

Dual-color ultraviolet metal-semiconductor-metal AlGaIn photodetectors


Appl. Phys. Lett. **89**, 143503 (2006); 10.1063/1.2358206

Nitride-based ultraviolet metal-semiconductor-metal photodetectors with low-temperature GaN cap layers and Ir/Pt contact electrodes



J. Vac. Sci. Technol. A **24**, 637 (2006); 10.1116/1.2162560

Very low dark current metal–semiconductor–metal ultraviolet photodetectors fabricated on single-crystal GaN epitaxial layers

Appl. Phys. Lett. **70**, 1992 (1997); 10.1063/1.118777



Instruments for Advanced Science

<p>Contact Hiden Analytical for further details: W www.HidenAnalytical.com E info@hiden.co.uk CLICK TO VIEW our product catalogue</p>	 <p>Gas Analysis</p> <ul style="list-style-type: none"> › dynamic measurement of reaction gas streams › catalysis and thermal analysis › molecular beam studies › dissolved species probes › fermentation, environmental and ecological studies 	 <p>Surface Science</p> <ul style="list-style-type: none"> › UHV TPD › SIMS › end point detection in ion beam etch › elemental imaging - surface mapping 	 <p>Plasma Diagnostics</p> <ul style="list-style-type: none"> › plasma source characterization › etch and deposition process reaction › kinetic studies › analysis of neutral and radical species 	 <p>Vacuum Analysis</p> <ul style="list-style-type: none"> › partial pressure measurement and control of process gases › reactive sputter process control › vacuum diagnostics › vacuum coating process monitoring
---	--	--	--	--

Performance enhancement of GaN metal–semiconductor–metal ultraviolet photodetectors by insertion of ultrathin interfacial HfO₂ layer

Manoj Kumar^{a)}

UNAM-National Nanotechnology Research Center and Institute of Materials Science and Nanotechnology,
 Bilkent University, 06800 Ankara, Turkey

Burak Tekcan and Ali Kemal Okay^{a)}

UNAM-National Nanotechnology Research Center and Institute of Materials Science and Nanotechnology,
 Bilkent University, 06800 Ankara, Turkey and Department of Electrical and Electronics Engineering,
 Bilkent University, 06800 Ankara, Turkey

(Received 19 September 2014; accepted 29 December 2014; published 9 January 2015)

The authors demonstrate improved device performance of GaN metal–semiconductor–metal ultraviolet (UV) photodetectors (PDs) by ultrathin HfO₂ (UT-HfO₂) layer on GaN. The UT-HfO₂ interfacial layer is grown by atomic layer deposition. The dark current of the PDs with UT-HfO₂ is significantly reduced by more than two orders of magnitude compared to those without HfO₂ insertion. The photoresponsivity at 360 nm is as high as 1.42 A/W biased at 5 V. An excellent improvement in the performance of the devices is ascribed to allowed electron injection through UT-HfO₂ on GaN interface under UV illumination, resulting in the photocurrent gain with fast response time. © 2015 American Vacuum Society. [<http://dx.doi.org/10.1116/1.4905735>]

I. INTRODUCTION

Owing to direct wide band gap, high saturation velocity and excellent thermal and chemical stability, GaN is considered one of the most promising semiconductor materials for ultraviolet (UV) photodetector (PD) application fields such as flame detectors, space to space detection and solar UV monitoring.^{1–3} Various types of UV PD structures based on GaN are examined and among them metal–semiconductor–metal (MSM) PD is a promising candidate due to its easy fabrication and compatibility with field effect transistor based electronics.^{4–8} However, the performances of GaN based PDs are still not up to the expectation, due to the excessive leakage current because of high dislocation densities that exist in the GaN thin films. Several developments such as AlGaIn/GaN metal-insulator-semiconductor PDs, AlGaIn on Si inverted Schottky PDs and inverted AlGaIn/GaN UV p-i-n PDs are demonstrated in this direction but most of them suffered from performance limitation especially low photoresponsivity.^{9–11} To facilitate further progress, it is vital to develop high responsivity PDs with inherent gain for detecting very low level light signal. Although, MSM PDs can exhibit internal gain that provides high responsivity, it is a slow process. Furthermore, the observed gain in GaN based MSM PDs is mainly caused by dislocation defects in the GaN thin films and existence of trapping states at the semiconductor and metal interface and are generally accompanied by large dark current and long response time. The utilization of interfacial insulating layer is an effective approach to suppress the leakage current and improve the device performance. Sang *et al.*¹² have proposed to utilize CaF₂ as an insulation layer to reduce dark current on InGaIn and succeeded to suppress dark current by 6 orders of magnitude in comparison to without CaF₂. Lee *et al.*¹³ have

suppressed dark current of GaN based UV PDs by depositing GaO_x in between metal and the GaN. Various insulating materials such as SiO₂, ZrO₂, and Al₂O₃ are reported.^{14–16} However, low dielectric constant (k) value restricts the maximum permissible electric field to the device. Therefore, high- k insulating material is helpful in reducing the field strength within the dielectric and thus allowing better performance of the devices. Moreover, it is essential for behaving perfect insulator on GaN, high k material band off set should exceed 1 eV and recent studies reveal that the interfacial layers also play an important role.¹⁷ HfO₂ is a suitable high- k material which has recently gained significant attention. In the present study, atomic layer deposition (ALD) grown UT-HfO₂ layer is inserted between metal and underlying GaN. The thickness of the HfO₂ layer is chosen as 1.5 nm so as not to produce any adverse effect on photocurrent. The dark current is observed to reduce more than 2 orders of magnitude and improved photo-to-dark current contrast ratio, and higher responsivity with internal gain. The dark and photocurrent studies are discussed in terms of carrier transport mechanism at the interface.

II. EXPERIMENT

The GaN samples used in this work were commercially available and grown using metal organic chemical vapor deposition technique on sapphire. The epilayer consisted of 1.2 μ m Si doped GaN and 300 nm unintentionally doped GaN. The nominal Hall Effect measured carrier concentration was found to be 1.4×10^{18} and 1.1×10^{17} cm⁻³, respectively. GaN samples were cleaned using acetone and isopropyl alcohol and then unintentionally grown oxide layer was etched by buffered hydrofluoric acid. Then, the insulating layer UT-HfO₂ was deposited on top of the GaN in Ultratech/Cambridge Nanotech Savannah 100 ALD system with tetrakis (dimethylamido) hafnium and H₂O as

^{a)}Authors to whom correspondence should be addressed; electronic addresses: panwarm72@yahoo.com; aokayay@ee.bilkent.edu.tr

precursors. The base pressure was maintained at 1 Torr during deposition.

Magnetron sputtered 10/100 nm thick Ni/Au interdigitated fingers (rectangular shaped of $5 \times 110 \mu\text{m}$ with spacing of $10 \mu\text{m}$) were directly fabricated on GaN. 10/100 nm thick Ni/Au and 100 nm thick Ni fingers were deposited on two batches of UT-HfO₂/GaN samples. The deposition was carried out in a vacuum chamber evacuated at base pressure of 5.6×10^{-6} Torr. High purity Ar was used as sputtering gas. During the Ni deposition power of 125 W, gas flow rate of 50 sccm, deposition time of 1 min, and pressure of 20 mTorr were kept constant. Au was fabricated at constant power of 75 W, gas flow of 50 sccm and pressure of 1 mTorr.

The current–voltage (I–V) measurements were performed using semiconductor parameter analyzer (Keithley 4200) and Keithley 2400 Sourcemeter. The spectral response was obtained by using a lock-in amplifier (SRS820) with an optical chopper and a monochromator from 300 to 420 nm with a 150 W xenon arc lamp. In order to measure photocurrent time response, a UV light source, a resistor of 100 Ω , and Keithley 2400 Sourcemeter were used.

III. RESULTS AND DISCUSSION

The typical room temperature dark and photo I–V characteristics of GaN MSM UV PDs without and with UT-HfO₂ prepared with different metal interdigitated fingers are illustrated in Fig. 1. The optical power of $36.89 \mu\text{W}$ at 360 nm UV illumination was kept constant during the measurements of photocurrent. It is clearly seen from Fig. 1 that devices with UT-HfO₂ interfacial layer dark current is reduced more than 2 orders of magnitude at a bias of 10 V. The Au/Ni/GaN device fabricated without UT-HfO₂ insertion exhibited dark current of 1.10×10^{-4} A; however, UT-HfO₂ introduced devices with different metal interdigitated fingers, namely, Ni/HfO₂/GaN and Au/Ni/HfO₂/GaN revealed dark current of 1.26×10^{-6} and 7.9×10^{-7} A, respectively, at a bias of 10 V. This demonstrates that UT-HfO₂ layer is an effective insulating layer for GaN based devices. Higher photo-to-dark current contrast ratios were also observed in both UT-HfO₂ inserted devices in comparison to without

UT-HfO₂ inserted device. As can be seen from Fig. 1 that the highest photo-to-dark current contrast ratio is provided by UT-HfO₂ inserted device with Au/Ni fingers at bias voltage of 5 V. It is supposed that UT-HfO₂ acts to highly suppress the surface defects, resulting in the reduction of recombination centers at the interface. This leads to a reduced dark current due to less thermal generation of carriers and increased photocurrent owing to higher collection efficiency with reduced recombination centers. It is suggested in the literature that introduction of thin insulation layer in-between metal and underlying semiconductor layer drastically reduced dark current and simultaneously decrease photocurrent as well. On the contrary, after insertion of UT-HfO₂ layer, photocurrent was found to increase. It is believed that UT-HfO₂ layer might have composed of either *coalescence*/island or dense nanoparticle over the GaN, which may scatter the incident light and thus increase the optical absorption and generate more electron-hole pairs. Sun *et al.*¹⁸ have effectively enhanced optical absorption efficiency after depositing SiO₂ nanoparticles on GaN surface. They have also observed that the dense nanoparticles further improved both electrical and optical properties of the GaN MSM UV PDs. Derkacs *et al.*¹⁹ also utilized SiO₂ nanoparticles for improving optical absorption efficiency in GaAs based solar cell.

Figure 2 shows responsivity spectra of GaN based MSM UV PDs without and with UT-HfO₂ insertion using different metal interdigitated fingers at a bias voltage of 5 V. All the devices clearly demonstrate relatively flat response at shorter wavelength side and sharp intrinsic transition above the band edge of GaN occurred at 360 nm. The measured peak responsivities of GaN MSM UV PDs without and with UT-HfO₂ layer prepared with Au/Ni, Ni, and Au/Ni interdigitated fingers were found to be 0.313, 0.47, and 1.42 A/W, respectively. The measured responsivities of all the devices are larger than the theoretical values (~ 0.29 A/W) of a GaN based PD, supporting presence of internal gain in the devices. It is clearly seen from Fig. 1 that the photogenerated current of UT-HfO₂ inserted UV PD prepared of Au/Ni interdigitated fingers is higher, thereby obtained the highest

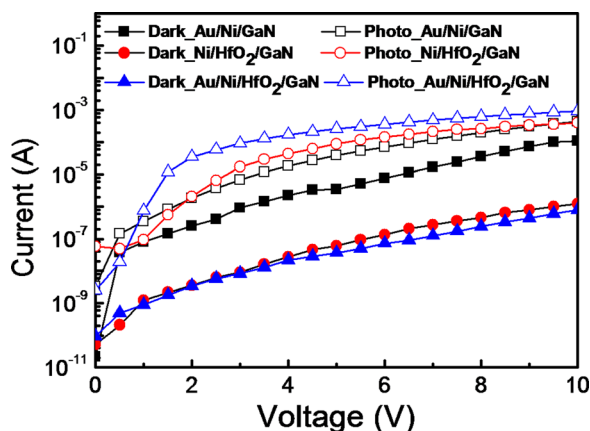


Fig. 1. (Color online) Typical room temperature dark and photo I–V characteristics of without and with UT-HfO₂ inserted in between metal and underlying GaN MSM UV PDS prepared with different interdigitated fingers.

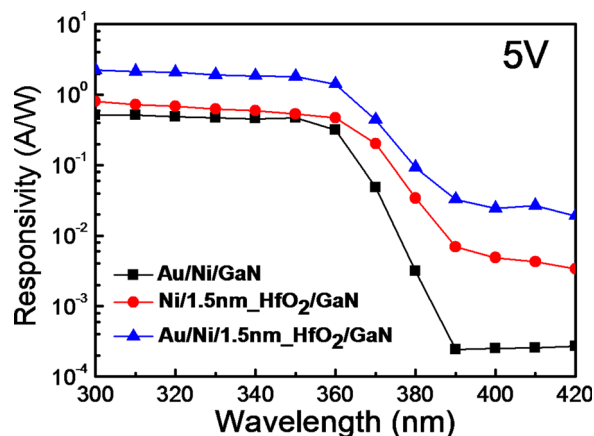


Fig. 2. (Color online) Spectral responsivity of MSM UV PDs fabricated without and with UT-HfO₂ inserted in between metal and underlying GaN prepared with different interdigitated fingers.

responsivity among the devices. UV to visible rejection ratio of GaN based MSM UV PDs without UT-HfO₂ insertion was obtained to be more than 3 orders of magnitude as defined the responsivity measured at 360 nm divided by that measured at 400 nm. However, it became smaller after introducing UT-HfO₂ interfacial layer, which may be due to high densities of defects introduced at the interface.

It is reported in the literature that Ni grows in pseudomorphic form when thickness is less than 10 nm and for higher thicknesses, FCC Ni is formed with many twins and stacking faults. In case of Ni-only metal electrode, Ni thickness was 100 nm. It is believed that FCC Ni is formed along with twins and stacking faults. Due to twins and stacking faults higher trap density exists at Ni/HfO₂ interface, which are responsible for electron capture. The captured electrons lead to the formation of a trapped electron charge space. These trapped electrons acts as hole traps and tend to capture photogenerated free holes from the GaN layer. Therefore, this trapping process increases the probability of the recombination of photogenerated carriers at the interface. On the other hand, for 10 nm Ni capped with Au, which not only prevents oxidation, but also improves conductivity of the contact during operation. Hence, Ni/Au metal electrode exhibits much better effect on improving the photocurrent responsivity of devices compared with Ni-only electrode.

Chen *et al.*²⁰ has reported that the spectral responsivity considerably increased after inserting a thin Si₃N₄ insulator layer. The significant improvement in responsivity after inserting a thin Si₃N₄ insulator layer is attributed to the enhancement of the effective surface barrier height and the reduction of the surface recombination loss. Si₃N₄ can reduce the density of defect states by surface passivation and hence decrease the probability of the surface recombination of photogenerated carriers. However, in the present study, formation of *coalescence*/island or dense nanoparticles of HfO₂ over the GaN layer, which terminate the dislocation defects. Thus, higher responsivity along with internal gain was obtained.

It is assumed that gain larger than theoretical value is related to charge trapping at the interface during illumination. It may be either thermionic field emission or tunneling model played major role for the carrier transportation. The thermionic field emission current density is given by²¹

$$J_{\text{TFE}} = J_s \exp\left(\frac{V}{E_0}\right) \left[1 - \exp\left(\frac{-qV}{kT}\right)\right], \quad (1)$$

$$E_0 = E_{00} \coth\left(\frac{E_{00}}{kT}\right), \quad (2)$$

$$E_{00} = \left(\frac{q\hbar}{2}\right) \left(\frac{N_t}{m^* \epsilon_s}\right)^{1/2}, \quad (3)$$

where q , N_t , m^* , and ϵ_s are elementary charge, carrier concentration, effective mass, and dielectric constant of the semiconductor, respectively. E_{00} reflects the tunneling probability. In the present case, $m^* = 0.22 m_0$ and $\epsilon_s = 9.5$ for GaN, and the carrier concentration N_t of the GaN film obtained by Hall measurement is about $1.0 \times 10^{17} \text{ cm}^{-3}$.

The estimated tunneling factor (E_{00}) was found to be 1.15 meV, which is much smaller than the thermal energy k_{BT} at room temperature (26 meV).

In order to investigate further the mechanism of the higher photoresponse phenomenon, the dark and photo I-V characteristic at forward bias were analyzed and the fitted I-V characteristics is shown in Figs. 3(a) and 3(b). It is interesting to note that different carrier transport mechanisms are dominant depending on applied voltage. It is found that Fowler–Nordheim (F-N) tunneling is the dominant conduction mechanism in all the devices at higher applied voltage. The F-N tunneling current is expressed by²²

$$J_{\text{FN}} = V^2 \exp\left(\frac{B}{V} + A\right), \quad (4)$$

where A and B are constants given by $A = q^2/(8\pi\hbar d^2\phi)$ and $B = 4(\sqrt{2}qm^*m_0\phi^{3/2}/3\hbar)$.

In the above equation, ϕ stands for the barrier height in eV, m^* is the effective electron mass, d is the tunnel barrier width, m_0 is the free electron rest mass, Q is the electron charge, and \hbar is the reduced Plank's constant. Figure 4 demonstrates the $\ln(I/V^2)$ vs $1/V$ F-N plot of forward dark and photo I-V characteristics of all the devices. At higher bias

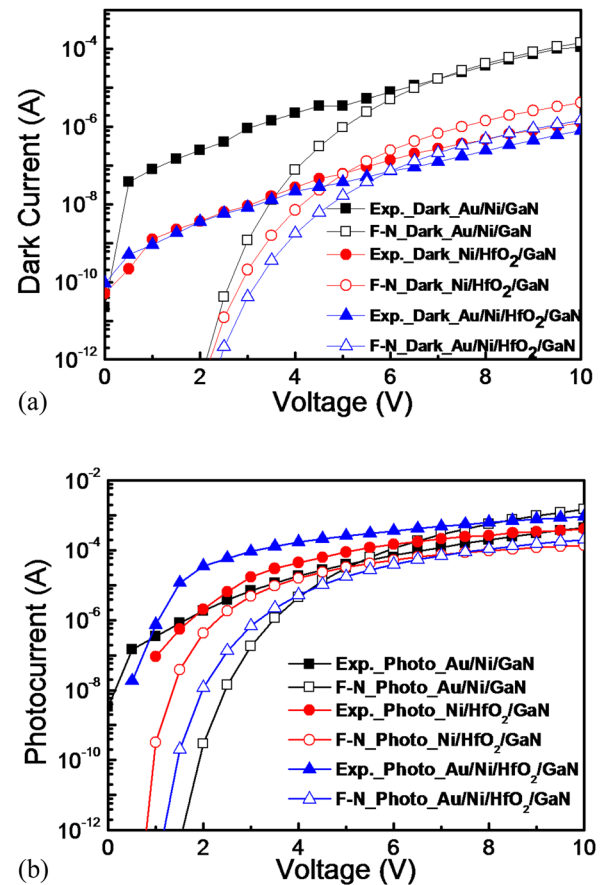


Fig. 3. (Color online) Fitting of forward (a) dark and (b) photo I-V characteristics by F-N tunneling of MSM UV PDS fabricated without and with UT-HfO₂ inserted in between metal and underlying GaN prepared with interdigitated fingers.

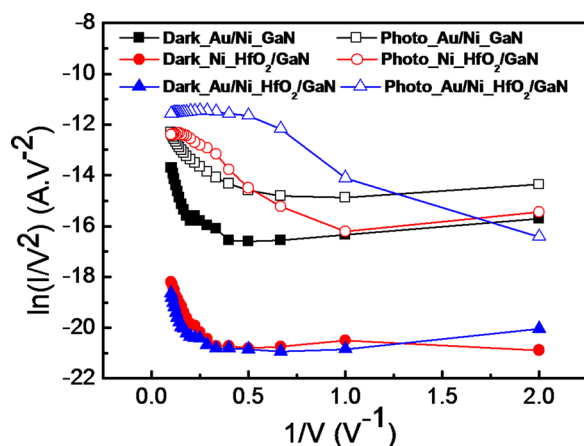


FIG. 4. (Color online) F-N plot of forward dark and photo I-V characteristics of MSM UV PDS fabricated without and with UT-HfO₂ inserted in between metal and underlying GaN prepared with different interdigitated fingers.

voltage $\ln(I/V^2)$ vs $1/V$ plot is found to linearly decrease having negative slope, which is a characteristics of F-N tunneling model. The F-N tunneling governs the photocurrent at higher applied voltage. It is also confirmed from fitting results that illuminated devices generates additional charge

of acceptor type traps close to the interface. The above analysis suggests that the observed gain is related to charge trapping at the interface during illumination. It can be realized that different carrier transport mechanism is dominated depending on applied voltage. At low bias voltage, the carrier transport is dominated by thermionic field emission whereas F-N tunneling is dominated at higher voltage.

The conduction band offset was calculated by F-N tunneling model and the valence band offset was obtained by $E_v = E_{\text{HfO}_2} - E_{\text{GaN}} - \phi_B$ where E_v , E_{HfO_2} , and E_{GaN} are the valence band offset and the band gap of HfO₂ and GaN, respectively.²³ The band diagram of without and with UT-HfO₂ devices prepared with different metal fingers are displayed in Fig. 5. The valence band offset value of the dark and illuminated device without UT-HfO₂ insertion was calculated as 1.69 and 1.79 eV, respectively. The photogenerated holes drifted toward the cathode are accumulated at the interface due to band bending. These accumulated holes are then captured by the surface states and some of them are trapped at the GaN surface because of existence of dislocation defects at the surface, which behaves as an acceptor like nature.²⁴ It is assumed that hole trapping causes electron swept out or re-injected in order to maintain charge

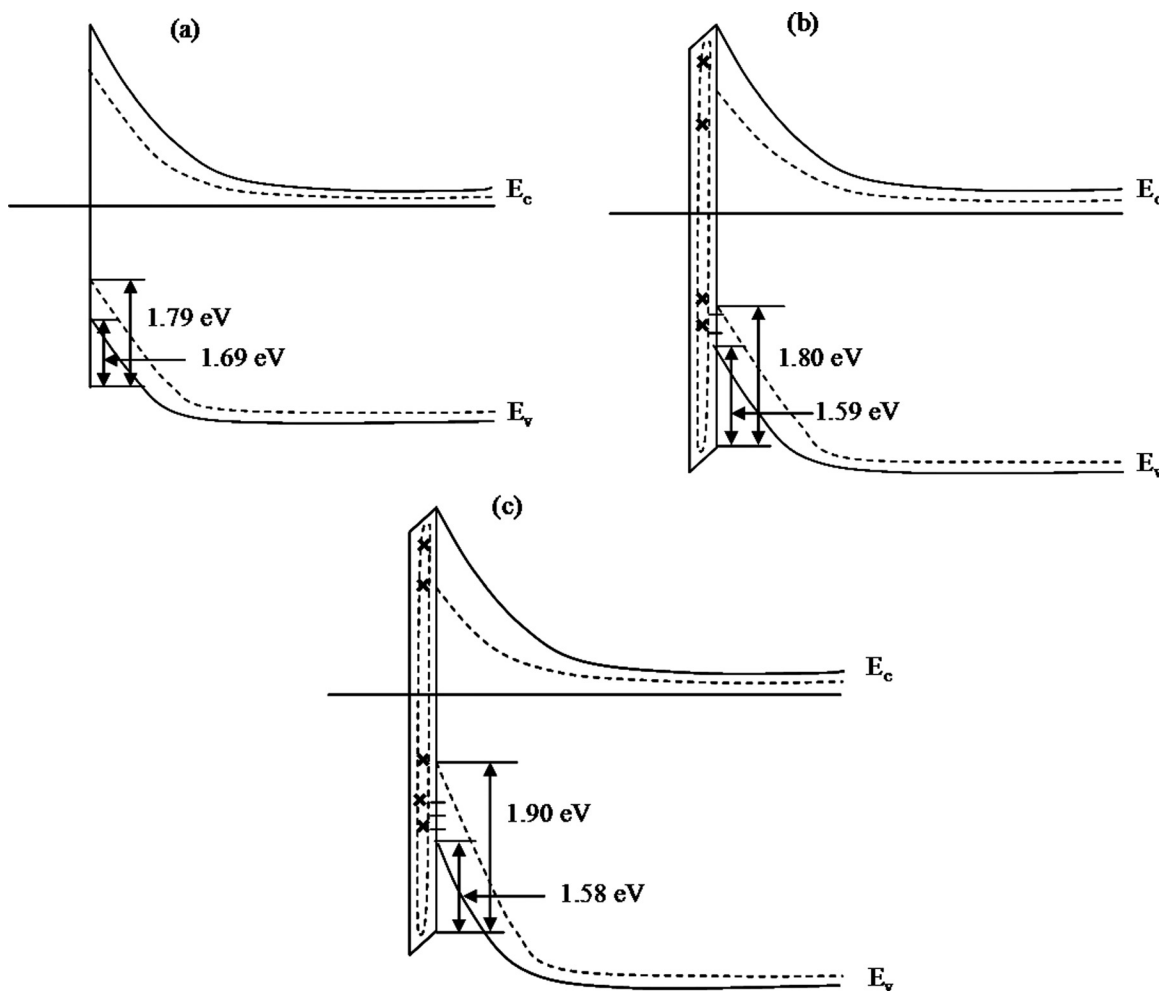


FIG. 5. Qualitative band diagram of (a) without HfO₂ inserted MSM UV PD prepared with Au/Ni interdigitated fingers, (b) with HfO₂ inserted MSM UV PD fabricated with Ni interdigitated fingers, and (c) with HfO₂ inserted MSM UV PD fabricated with Au/Ni interdigitated fingers.

neutrality in the space charge region. This action is responsible for observed gain in the device. The calculated valence band offsets of the devices inserted with UT-HfO₂ and prepared with Ni and Au/Ni metal fingers are obtained as 1.80 and 1.90 eV, respectively, which is higher than that of without UT-HfO₂ inserted device. The UT-HfO₂ inserted device prepared with Au/Ni finger exhibited maximum valence band offset, leading larger number of holes to accumulate and get trapped at the interface and produces the highest responsivity with internal gain. It is widely recognized that the occurrence of gain in the GaN based devices is associated with longer life-time of photogenerated holes.²⁵ The longer life-time of holes is usually induced by trapping either at interface or on the surface of the active layer. Interface states occur during device formation. It is justified that the occurrence of gain in the present study is due to hole trapping, resulting in electrons being swept out rapidly and circulating many times through external circuit before recombining with holes. It is observed that gain appeared in the device fabricated without UT-HfO₂ accompanied by a slow time response as shown in inset of Fig. 6; on the other hand, the devices prepared with UT-HfO₂ revealed fast time response despite higher gain. The obtained high response speed might be due to relative shallow energy level of trapped holes. Deeper traps have longer charge release time and thus result in a slower device response. It is mentioned in the literature that the PD response speed is related to the trap occupancy, which depends on light intensity. At low intensity, the photocurrent decay is expected to be dominated by the slower process, because deeper traps are easier to be field. Time response was also measured with low (10 μ W) and high power intensity (36 μ W) and the device without UT-HfO₂ interfacial layer revealed slow response however, UT-HfO₂ inserted devices exhibited fast responses with low and high power intensity (low power intensity data are shown here). The assurance of fast response of UT-HfO₂ inserted devices with low and high power intensity suggests that either tiny or no deep traps are generated by introducing UT-HfO₂ layer.

These features denote that UT-HfO₂ plays crucial role in controlling the photoresponse of the GaN MSM UV PDs and

it performs an effective insulation in the dark condition, which reduces the influence of dislocation defects and suppress the dark current. Furthermore, it enhanced light absorption on the active layer, thereby device performance improved. The measurements were also repeated at a certain time interval to test the reproducibility of the devices and every time similar results were obtained.

IV. CONCLUSION

In conclusion, we have investigated dark and photocurrent characteristics of without and with UT-HfO₂ inserted GaN UV PDs. Introducing UT-HfO₂ interfacial layer reduced dark current more than two orders of magnitude and increased the photocurrent. The device prepared with Au/Ni fingers on UT-HfO₂ inserted GaN UV PD exhibit the highest responsivity of 1.42 A/W at wavelength of 360 nm and applied bias of 5 V. The UT-HfO₂ inserted devices maintained fast response time in spite of showing gain. The present results demonstrate that UT-HfO₂ is a potential candidate for insulation of GaN based UV PDs and optoelectronic devices.

ACKNOWLEDGMENTS

This work was supported by the Scientific and Technological Research Council of Turkey (TUBITAK), Grant Nos. 109E044, 112M004, 112E052, and 113M815. A.K.O. acknowledges support from European Union FP7 Marie Curie International Reintegration Grant (PIOS, Grant No. PIRG04-GA-2008-239444). A.K.O. acknowledges support from the Turkish Academy of Sciences Distinguished Young Scientist Award (TUBA GEBIP).

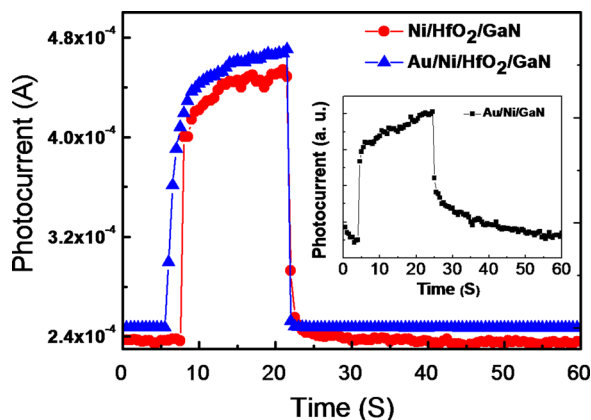


Fig. 6. (Color online) Time response spectra of without HfO₂ inserted layer prepared with Au/Ni interdigitated fingers (inset) and with HfO₂ inserted MSM UV PDS fabricated with Ni and Au/Ni interdigitated fingers.

- ¹D. Walker, A. Saxter, P. Kung, X. Zhang, M. Hamilton, J. Diaz, and M. Razeghi, *Appl. Phys. Lett.* **72**, 3303 (1998).
- ²G. Hellings, J. John, A. Lorenz, P. Malinowski, and R. Mertens, *IEEE Trans. Electron Devices* **56**, 2833 (2009).
- ³M. Asif Khan, M. Shatalov, H. P. Maruska, H. M. Wang, and E. Kuokstis, *Jpn. J. Appl. Phys., Part 1* **44**, 7191 (2005).
- ⁴B. W. Lim, Q. C. Chen, J. Y. Yang, and M. Asif Khan, *Appl. Phys. Lett.* **68**, 3761 (1996).
- ⁵Q. Chen, J. W. Yang, A. Osinsky, S. Gangopadhyay, B. Lim, and M. Z. Anwar, *Appl. Phys. Lett.* **70**, 2277 (1997).
- ⁶R. Hickman *et al.*, *Solid-State Electron.* **44**, 377 (2000).
- ⁷Y. Kang, Y. Xu, D. Zhao, and J. Fang, *Solid-State Electron.* **49**, 1135 (2005).
- ⁸D. Yoo, J. Limb, J.-H. Ryou, Y. Zhang, S.-C. Shen, R. D. Dupuis, D. Hanser, E. Preble, and K. Evans, *IEEE Photonics Technol. Lett.* **19**, 1313 (2007).
- ⁹P. C. Chang, C. H. Chen, S. J. Chang, Y. K. Su, C. L. Yu, B. R. Huang, and P. C. Chen, *Thin Solid Films* **498**, 133 (2006).
- ¹⁰P. E. Malinowski *et al.*, *Appl. Phys. Lett.* **98**, 141104 (2011).
- ¹¹K. H. Chang, J. K. Sheu, M. L. Lee, S. J. Tu, C. C. Yang, H. S. Kuo, J. H. Yang, and W. C. Lai, *Appl. Phys. Lett.* **97**, 013502 (2010).
- ¹²L. Sang, M. Liao, Y. Koide, and M. Sumiya, *Appl. Phys. Lett.* **98**, 103502 (2011).
- ¹³M. L. Lee, T. S. Mue, F. W. Huang, J. H. Yang, and J. K. Sheu, *Opt. Express* **19**, 12658 (2011).
- ¹⁴C. H. Chen, Y. H. Tsai, S. Y. Tsai, and C. F. Cheng, *Jpn. J. Appl. Phys., Part 1* **50**, 04DG19 (2011).
- ¹⁵Y. Z. Chiou, *J. Electrochem. Soc.* **152**, G639 (2005).
- ¹⁶C. J. Lee, Y. J. Kwon, C. H. Won, J. H. Lee, and S. H. Hahma, *Appl. Phys. Lett.* **103**, 111110 (2013).
- ¹⁷C. H. Chen, *Jpn. J. Appl. Phys., Part 1* **52**, 08JF08 (2013).

- ¹⁸X. Sun, D. Li, H. Jiang, Z. Li, H. Song, Y. Chen, and G. Miao, *Appl. Phys. Lett.* **98**, 121117 (2011).
- ¹⁹D. Derkacs, W. V. Chen, P. M. Matheu, S. H. Lim, P. K. L. Yu, and E. T. Yu, *Appl. Phys. Lett.* **93**, 091107 (2008).
- ²⁰D. J. Chen, B. Liu, H. Lu, Z. L. Xie, R. Zhang, and Y. D. Zheng, *IEEE Electron Device Lett.* **30**, 605 (2009).
- ²¹Z. Q. Shi and W. A. Anderson, *Solid-State Electron.* **34**, 285 (1991).
- ²²M. Liao, X. Wang, T. Teraji, S. Koizumi, and Y. Koide, *Phys. Rev. B* **81**, 033304 (2010).
- ²³F. Zhang *et al.*, *IEEE Electron Device Lett.* **32**, 1722 (2011).
- ²⁴L. Leung, A. F. Wright, and E. B. Stechel, *Appl. Phys. Lett.* **74**, 2495 (1999).
- ²⁵M. M. Fan, K. W. Liu, Z. Z. Zhang, B. H. Li, X. Chen, D. X. Zhao, C. X. Shan, and D. Z. Shen, *Appl. Phys. Lett.* **105**, 011117 (2014).